

Effects of burner configurations on the natural oscillation characteristics of laminar jet diffusion flames

K. R. V. Manikantachari, Vasudevan Raghavan and K. Srinivasan

Department of Mechanical Engineering, Indian Institute of Technology Madras, Chennai

(Submission date: July 30, 2014; Revised Submission date: November 21, 2014; Accepted date: January 05, 2015)

ABSTRACT

In this work, effects of burner configurations on the natural oscillations of methane laminar diffusion flames under atmospheric pressure and normal gravity conditions have been studied experimentally. Three regimes of laminar diffusion flames, namely, steady, intermittent flickering and continuous flickering have been investigated. Burner configurations such as straight pipe, contoured nozzle and that having an orifice plate at the exit have been considered. All burners have the same area of cross section at the exit and same burner lip thickness. Flame height data has been extracted from direct flame video using MATLAB. Shadowgraph videos have been captured to analyze the plume width characteristics. Results show that, the oscillation characteristics of the orifice burner is significantly different from the other two burners; orifice burner produces a shorter flame and wider thermal plume width in the steady flame regime and the onset of the oscillation/flickering regimes for the orifice burner occurs at a higher fuel flow rate. In the natural flickering regime, the dominating frequency of flame flickering remains within a small range, 12.5 Hz to 15 Hz, for all the burners and for all fuel flow rates. The time-averaged flame length-scale parameters, such as the maximum and the minimum flame heights, increase with respect to the fuel flow rate, however, the difference in the maximum and the minimum flame heights remains almost constant.

1. INTRODUCTION

Laminar jet diffusion flames exhibits three regimes of burning, depending upon the fuel flow rate. They are steady burning regime, regime with intermittent oscillations/flickering and continuous flickering regime. Flame appears to be almost steady when the fuel flow rate is less than a certain value. It starts to flicker after that flow rate; however, the flickering is not continuous. The flame seems to be steady during some time period and sometimes oscillatory. At a still higher flow rate, the

*Corresponding author: raghavan@iitm.ac.in

intermittent flickering regime transits to continuous flickering/oscillating regime, where the flickering phenomenon becomes continuous. The interactions of vortices in the flow field with the reaction zone play a key role in flame oscillations. These interactions can basically alter the mixing phenomena and can lead to flickering of the flames and related instabilities. Studies to understand the flickering of diffusion flames, which occur either naturally or due to external disturbances, are very important in burner and furnace designs. In general, a better understanding of flickering process provides insights to the characteristics of the turbulent flames as such instability can grow rapidly in the presence of a turbulent flow.

There are several studies available, where flame oscillation or flickering process has been examined using various parameters. Earlier studies showed that a naturally occurring flame-vortex interaction is typically periodic, generally regular and reproducible (Grant and Jones [1], Chamberlin and Rose [2]). Hamins et al. [3] experimentally analyzed the minimum velocity (fuel flow rate) required for the onset of flame flickering as a function of burner diameter. It has been reported by Maxworthy [4] that depending upon the fuel flow rate, three flickering regimes, steady, intermittent and continuous, are observed in candle flames. Further research studies are available in which the flickering characteristics of the flames have been investigated in detail using different fuel types (Li and Zhang [5]), gravity levels (Sato et al. [6]), surrounding pressure (Darabkhani and Zhang [7]), with co-flowing air (Darabkhani et al. [8]) and with acoustic excitations (Huang et al. [9]).

Research studies, which examine the reasons for flame flickering, are also available. Kimura [10] and Toong et al. [11] concluded that the flame oscillations are triggered by Tollmien-Schlichting waves, which is the same mechanism that triggers the transition of laminar to turbulent flows. However, the invariance of oscillation frequency with respect to fuel flow rate was not explained by that theory. Buckmaster and Peters [12] theoretically predicted the invariance of flickering frequency, however, by uncoupling the effect of fuel flow rate. Flame flickering was shown as a pure buoyancy induced phenomenon, which was not related to flow induced instabilities. Davis et al. [13] and Katta and Roquemore [14] also supported the phenomenon of buoyancy induced instabilities as the reason for the onset of flame flickering. Bounager [15] summarized the flame flickering mechanism as follows: the heat release due to combustion results in increase in temperature of the gases in the vicinity of the flame (reaction zone) surface. A temperature gradient forms from the flame surface towards the ambient. Since the density is inversely proportional to temperature, the gas near flame surface experiences more buoyancy force and rises up. This causes a suction effect and relatively cold gas entrains, creating a couple (torque) on the local lump of gases. As a result, the gas lump rolls up leading to the formation of vortices. These vortices are responsible for the periodic elongation of flame and shedding of its tip subsequently. Various modes in which the flame flickers is due to the gradient in the buoyant plume density around the flame surface towards the cold ambient.

Studies by past researchers that categorize the flame flickering modes are also available. Cetegen and Dong [16] reported that under normal ambient conditions when the flame continuously flickers, there are two oscillation modes, varicose mode with

axial flame oscillations, and sinuous modes, in which the flame bends to form an 'S' shape. Sato et al. [6] reported about two types of flame flickering namely, tip flickering, where the flame tip does not separate while oscillating, and bulk flickering, where the flame tip gets separated (sheds) from the bulk flame while oscillating.

A recent preliminary study by Manikantachari et al. [17] reported that the onset of the flame flickering occurs at fuel flow rates that are also dependent on internal flow configurations of the burner, apart from the burner diameter as shown by Hamins et al. [3]. For the same exit diameter of the burner, the minimum velocity required to initiate the flickering process differs, based on the configuration of the burner. For instance, the burner with an orifice plate at the exit is seen to suppress the flickering until higher fuel flow rates than a nozzle or a pipe burner with the same exit diameter. However, the occurrence of the various modes, as reported by Cetegen and Dong [16] and Sato et al. [6], and the reasons for the mode shifting process are not reported in detail.

In summary, researchers have reported adequate numerical and experimental works on the natural flickering of diffusion flames. However, studies on the effects of burner geometry on flame flickering and results for detailed understanding of the transition from one regime to the other and from one mode to the other are scarce. Current work attempts to investigate the effects of the burner internal geometry on the oscillations characteristics of methane diffusion flames and to understand their behaviour in steady, intermittent flickering and continuous flickering regimes in detail.

2. EXPERIMENTAL SETUP AND PROCEDURE

Three burners, as shown in Fig. 1, are made of brass. The exit diameter, burner height and lip thickness of the three burners are kept the same (5 mm, 50 mm and 3 mm, respectively). The internal geometries have been varied as in Fig. 1, to get (a) circular nozzle, (b) straight pipe and (c) orifice plate burners. These burners are fastened to a settling chamber, shown in Fig. 1 (d). A schematic representation of overall experimental setup is shown in Fig. 2. Two metal meshes are placed inside the settling chamber to cut down the eddies. Methane is supplied through a mass flow controller (Aalborg; Model GFC17-07). The flow rate of methane is varied in a range so as to cover all the three regimes of flame oscillations. A thermocouple of (K-type) with a wire diameter of 0.27 mm is used for measuring the temperature distribution around the flame. Temperature has been recorded using a data logger of resolution 0.1°C. High speed video of the diffusion flame is captured by using a digital camera (Casio EX-F1). The ISO sensitivity and focus are set appropriately with respect to the lighting and the zoom level.

The images are acquired at a rate of 300 frames per second. Captured videos are converted to stack of frames by using image processing software called ImageJ. The digital images, thus obtained, are processed using a MATLAB code to measure the flame height with respect to the burner base. The temporal flame height data is converted to the frequency domain using Fast Fourier Transform (FFT). Apart from direct flame images, shadowgraph images are also recorded in a single setting using the optical setup shown in Fig. 2. Each experiment is repeated at least 3 times to check for the consistency.

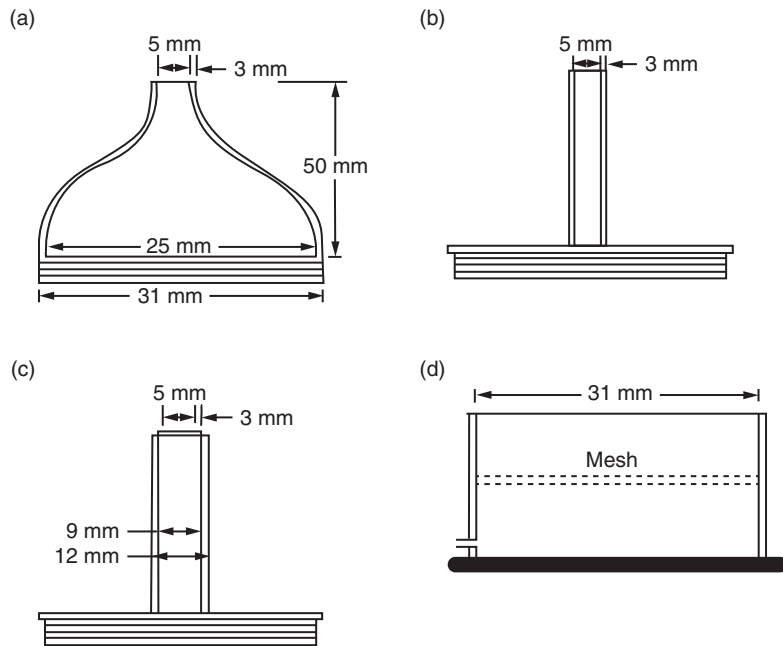


Figure 1: Schematic diagrams of the burners and the settling chamber.

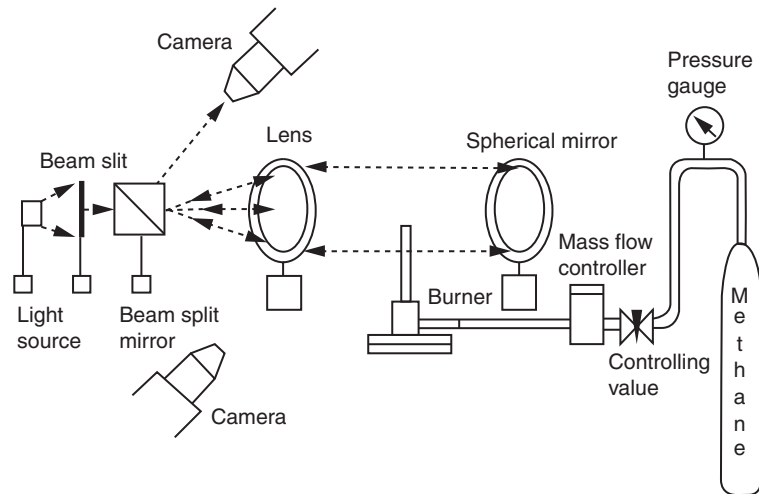


Figure 2: Schematic diagram of the experimental setup.

3. RESULTS AND DISCUSSIONS

3.1. Numerical investigation of exit velocity and jet half width profiles

It is important to distinguish between the resultant flow fields from the three types of burners shown in Fig. 1. Since reacting flow simulations are very complex, in this study, two-dimensional axisymmetric steady cold flow simulations have been carried out using commercial CFD software FLUENT for air flow rates of 200 mlpm, 410 mlpm and 610 mlpm. The flow development processes inside the burners and the characteristics of the jets expanding in to the free ambience have been modeled using laminar flow simulations and standard model parameters available in FLUENT. Mass flow inlet, far-field pressure and axis of symmetry have been chosen as the boundary conditions.

The mean stream-wise velocity profiles at the exit plane depend on the internal flow development within the burner. This exit velocity profile dictates the further jet characteristics, one of which is the jet half-width variation along the axial direction. Figure 3 shows the axial velocity profiles at the burner exit (left) and the variation of jet half-width in the axial direction (right) for the three burners. It is apparent that the flow characteristics of orifice jet are much different. It has a higher value of jet half-width than the other two burners, especially when the volumetric flow rate is higher. This indicates that the mixing characteristics of the orifice jet are better.

3.2. Steady flame regime

3.2.1. Radial temperature distribution outside the flame zone

In a reactive jet, there is a steep temperature gradient in the radial direction. This in turn creates an imbalance of the local mass in the vicinity of the hot flame zone due to buoyancy effects. This imbalance further develops as a vortex roll-up and interacts with flame [15]. For the three burners, under steady flame regime and for the same fuel flow rate, temperature distributions around the flame have been measured. Thermocouple has not been placed inside the visible flame zone to avoid any disturbances to the flame. The objective of this measurement is to provide the radial temperature decay for the three burners, which would indicate the relative strengths of the vortices. Further, this exercise has not been carried out for flickering regimes, as there are increased uncertainties involved in the temperature measurements when the flame flickers.

Convection and radiation losses have been accounted to correct the raw temperature data. The thermocouple is placed at different radial locations (between 8 mm to 18 mm from the burner axis) and at two axial locations, one at the burner exit and another around 15 mm from the burner exit. To ensure the repeatability of the measurements, experiment is repeated thrice, and a fluctuation ± 15 K is observed in the measurements. The radial temperature profiles at the two axial locations are shown in the Figs. 4(a) and 4(b), for the fuel flow rate of 200 mlpm (milliliters-per-minute), which produces visible steady flames in all the three burners. This corresponds to a Reynolds number of 74, calculated for methane based on the burner exit diameter and average jet velocity. It is clear that the radial temperature distributions in the cases of pipe and nozzle burners are almost the same and that in the case of the orifice burner is quite different; the temperature values are higher than the other two cases. Further, the decay of

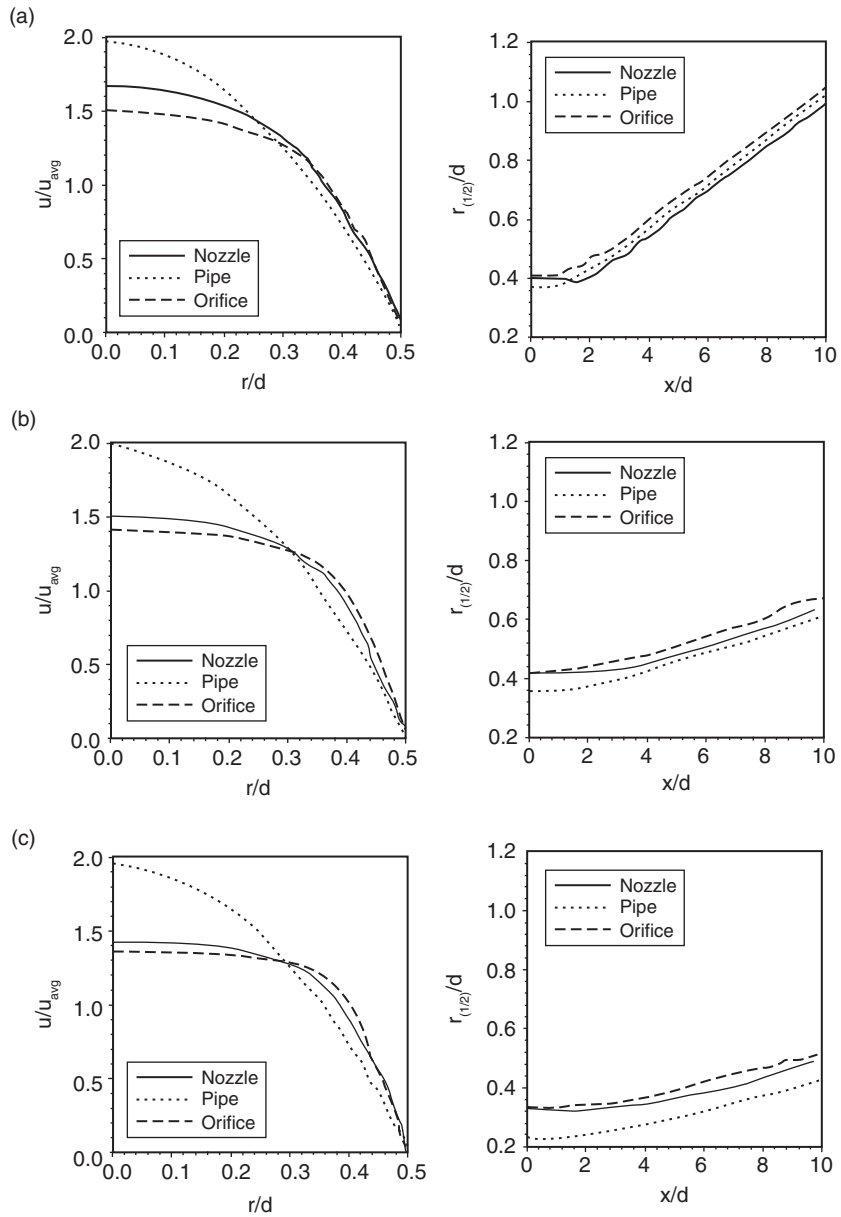


Figure 3: Predicted axial velocity profile at burner exit (left) and jet half width along the axis (right) for three burners at air flow rates of (a) 200 mlpm, (b) 410 mlpm and (c) 610 mlpm.

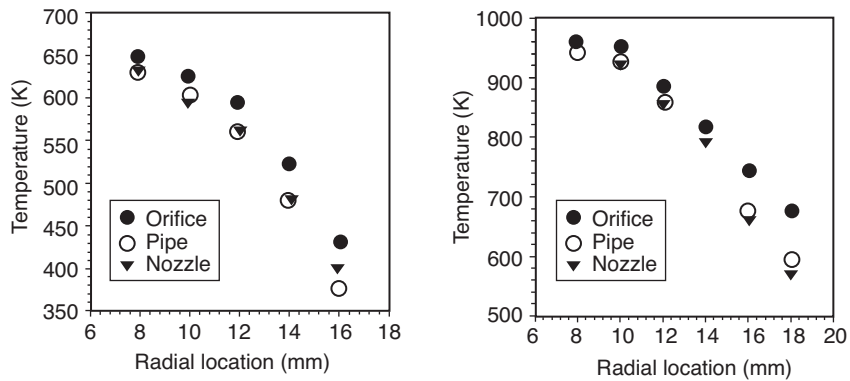


Figure 4: Radial temperature distributions for different burners for the fuel flow rate of 200 mlpm ($Re = 74$) at the burner exit (left) and 15 mm away from the burner exit (right).

temperature along the radial direction is observed to be slower in the case of orifice burner. Even though the temperature distribution at higher flow rates have not been measured due to higher temperature fluctuations in those cases, the trends observed in the steady regime indicate that the time averaged mean temperature distribution can be expected to be similar as presented in Fig. 4. As discussed earlier, the buoyancy force acting on a local mass of gas in the flame vicinity is directly proportional to the temperature gradient. Lesser the temperature gradient weaker will be vortices, if formed. A weaker vortex does not have sufficient energy to interact with the flame and cause the flame to fluctuate. Therefore, the case of orifice burner can be expected to be more steady than the other two burners. The strength of the vortices increases with respect to increase in fuel flow rate. However, due to the trend shown in Fig. 3, there is an expected delay in the flame flickering in the case of the orifice burner, as explained by Cetegen and Dong [16], due to the slower decay of radial temperature profile.

3.2.2. Comparison of flame height

The flame height is the one of the main characteristics of the jet diffusion flame. In the laminar regime, the flame height is proportional to the volumetric flow rate of the fuel. For circular ports, various combinations of exit velocity and burner diameter providing the same fuel volume flow rate result in the same flame height. However, when burner exit configurations vary, even for the same exit diameter and superficial velocity, that is, for the same volume flow rate, the average flame heights are observed to be different. In the cases of straight pipe, contoured nozzle and orifice burners, the internal flow development and exit velocity profile will vary, and as a result, the entrainment and mixing characteristics change. High-definition direct flame images are captured with a shutter speed of 0.5 s for these three cases for the fuel flow rate of 200 mlpm. Figure 5 shows time averaged images of the flames from three burners. The visible flame heights are measured from these images, using an image processing tool called ImageJ. The

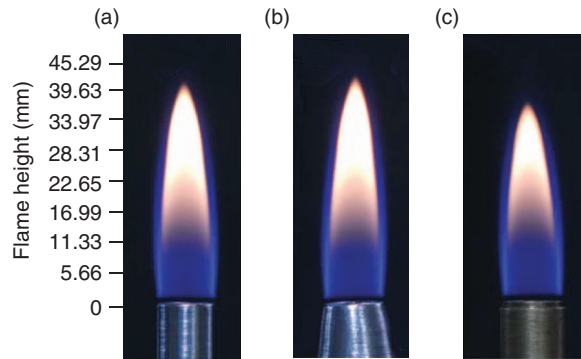


Figure 5: Time averaged digital photographs of flames for fuel flow rate of 200 mlpm ($Re = 74$) in (a) straight pipe, (b) nozzle, and (c) orifice burners.

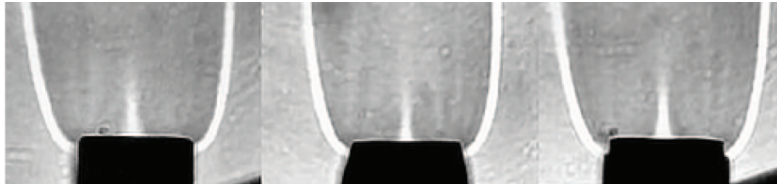


Figure 6: Near field shadowgraph images of flames shown in Fig. 4 ($Re = 74$).

flame height value is estimated within an uncertainty of ± 0.5 mm. The average flame height in steady regime in case of orifice burner exit condition is around 36.5 mm. This is around 10% less than the averages heights in the nozzle burner (39 mm) and in the straight pipe burner (39.5 mm). The abrupt change in the boundary layer growth within the burner and the resulting velocity profile at the burner exit, contributes to this change. A short flame is not affected by vortices generated downstream (Boulnager [15]) and the shorter flame height in the case of the orifice burner forms another reason for why the flame flickering phenomenon occurs at higher fuel flow rate. Shorter flames are less affected by the vortices in the flow field.

3.2.3. Thermal plume characteristics

The shadowgraph images in the near field of the flames presented in Fig. 5 are shown in Fig 6. These images show the second derivative of density with respect to space. The width of the thermal plume around the flame indicates the relative strength of entrainment. In the shadowgraph images, black regions represent the burner shadow. The maximum intensity (white) lines show the preheat region in the air (outer white lines) and fuel sides (inner white cone). It is reported that when the mixing is enhanced, the preheat lines move away from the flame surface because of the enhanced transport of heat towards the air-side from un-burnt fuel (Kanthasamy et al. [18]). The enhanced heat transport is due to the enhanced entrainment of air.

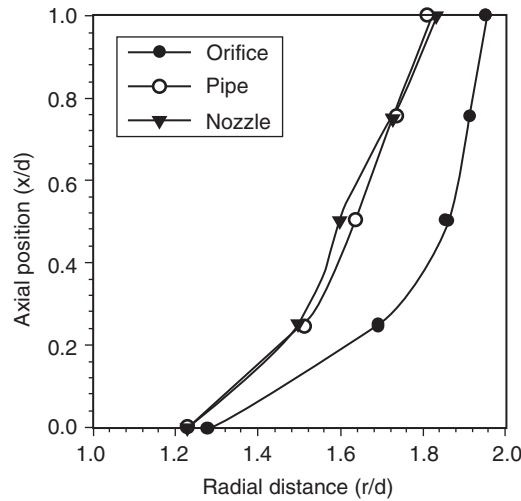


Figure 7: Variation of thermal plume width/radius along the flame axis for the cases shown in Fig. 6.

The shadowgraph images show that the thermal plume around the flame originates at location just below the edge of the burners (Fig. 6). The radial widths of the thermal plume (distance between the axis of the burner to the outer edge of the thermal plume) in the shadowgraph images for the three burners have been obtained at different axial locations by image processing using a MATLAB code and are plotted in Fig. 7. It is apparent that entrainment behavior in the case of orifice burner is quite different, with a maximum difference in the plume width around 1.2 mm (Fig. 7), as compared to other two burners, which behave almost similarly.

3.2.4. Low amplitude flickering in steady flame regime

In the steady flame regime, even though the diffusion flame appears to be steady (visually the height of the flame appears to remain constant with time), through the image processing of the digital flame images, it has been observed that very low amplitude oscillations are present in this regime as well. The videos of the flames from three burners are recorded keeping the fuel flow rate as 200 mlpm for a time period of three minutes, at a rate of 300 frames per second. The videos are converted into frames (573×384) and are processed in MATLAB to acquire flame height data at regular time intervals. As mentioned earlier, the flame height is calculated within an uncertainty of ± 0.5 mm. The temporal variations of the flame heights for the three cases are shown in Fig. 8. These plots present the analysis from 54000 frames each. The time averaged digital flame images of these flames are shown in Fig. 4. The variation in the flame height for each case with respect to corresponding mean is in the range of ± 2 mm maximum.

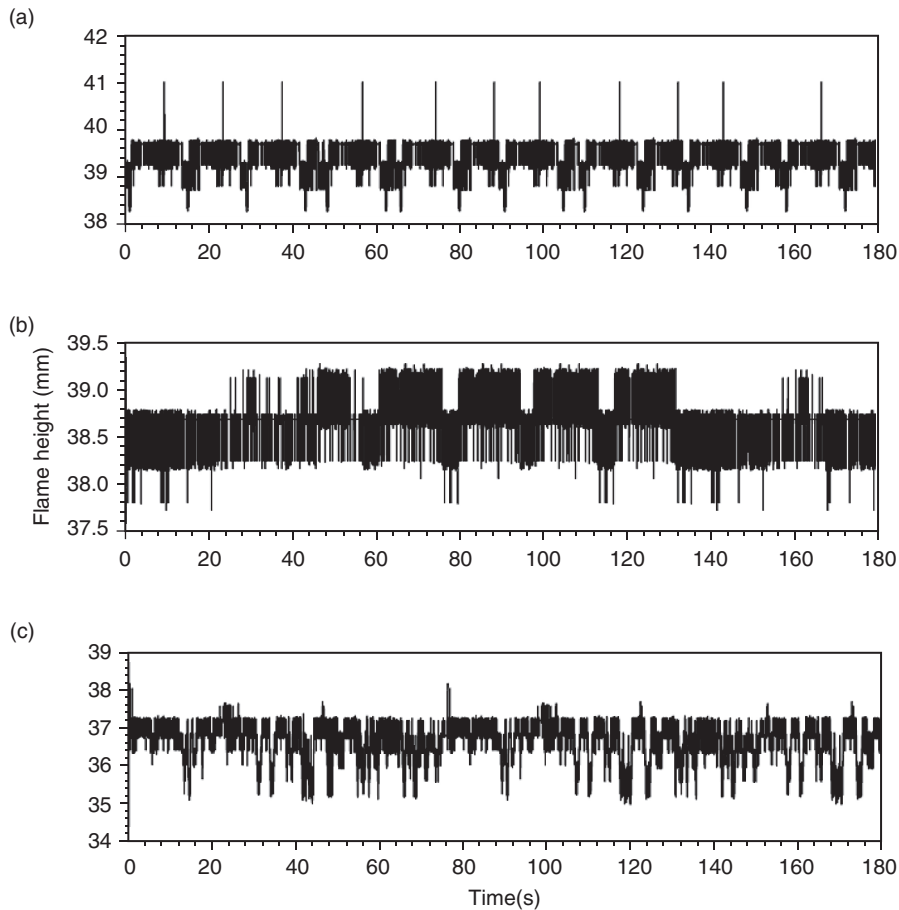


Figure 8: Flame height variations with time for a fuel flow rate of 200 mlpm ($Re = 74$) for different burners; (a) pipe, (b) nozzle and (c) orifice.

3.3. Intermittent flickering regime

As the fuel flow rate is increased gradually, based on the burner configuration, the flame starts to flicker. Initially as the onset of flickering has occurred, the flickering process does not occur continuously. The flame remains steady for some time-period and flickers during another time-period. In addition, the time-periods at which flickering occurs are not uniform. In the intermittent flickering regime, the flame becomes sensitive to certain disturbances in the flow field. These disturbances lead to flame flickering for some time-period and eventually the flame regains its steadiness once the reactive zone could overcome the strength of the disturbances.

Maxworthy [4] defined a useful parameter, termed intermittency, for representing the oscillating condition (steady or fluctuating) for the jet diffusion flame. This parameter quantifies phenomenon of alteration in the state of the flame between steady and periodic regimes. This is quite different from the dynamical systems theory, where intermittency represents only the phenomenon of alteration of system state between periodic to chaotic phases. Therefore, the term intermittency used in this study is defined as the percentage of the time when the flame is flickering in a certain long enough time-period of observation. This is mathematically represented in equation (1). For example, if the flame is completely steady, then the flickering time is zero and the Intermittency will also be zero. On the other hand, if the flame is flickering continuously, then the value of intermittency will be hundred. In the intermittent flickering regime, the value of intermittency will be in between 0 and 100.

$$\text{Intermittency (\%)} = \text{Total flickering time} \times 100 / \text{Total observation time} \quad (1)$$

3.3.1. Variation of intermittency with fuel flow rate

The flame behavior is recorded for three minutes at a rate of 300 frames per second. These videos are then processed to make an estimate of the percentage of time when the flame has been flickering during the total time. The value of intermittency as a function of fuel flow rate is shown in Fig. 9 for all the three burners. Figure 9 illustrates that at low flow rates, in the steady flame regime, neglecting the low amplitude oscillations which are not visually captured, the value of intermittency is zero. Corresponding to the burner configuration, when the fuel flow rate is gradually increased, at a certain fuel flow rate, the value of intermittency starts to increase gradually. This represents the

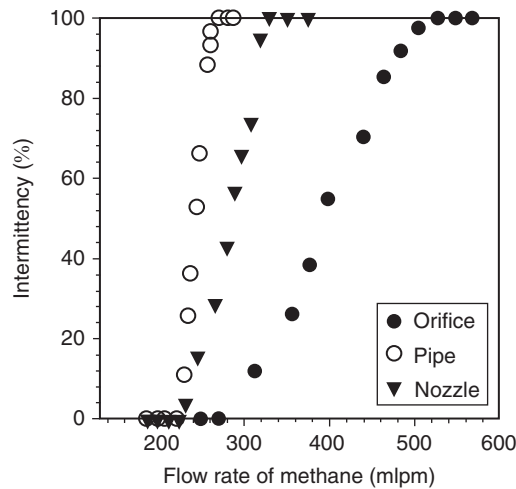


Figure 9: Variation of the intermittency of the flickering flame with respect to the fuel flow rate for three burner configurations.

onset of the intermittent flickering regime. At a certain higher flow rate, dependent on the burner type, intermittency reaches the value of unity, where the onset of continuous flickering regime is observed. It is clear from Fig. 9 that for pipe burner, the onset of initial flickering occurs around a fuel flow rate of 225 mlpm and for nozzle burner it is around 230 mlpm. However, for the orifice burner, the onset of initial flickering occurs at a much higher fuel flow rate, around 290 mlpm. This trend for orifice burner is consistent with the observation of Cetegen and Dong [16]. Intermittent flickering is a transition regime, where the increased inertia of the jet could both initiate as well as suppress the external disturbances in the surrounding flow field and this process continues up to a point where the external flow field could completely influence the flame zone as in continuous regime.

3.3.2. Flame flickering modes in intermittent flickering regime

Flame flickering from the three burners has been classified as varicose flickering and sinuous flickering modes, in the preliminary study presented by Manikantachari *et al.* [17]. From the results of this study, these two classes can be further sub-divided into four other modes such as, varicose bulk flickering, varicose tip flickering, sinuous bulk flickering and sinuous tip flickering. During a bulk-flickering mode, the flame-tip is separated while flickering. On the other hand, there is no flame tip separation during a tip flickering process. In the Sinuous mode of flickering, the flame becomes asymmetric and in the varicose mode, it is symmetric. Not all these modes can be observed in all the three flickering regimes. Based on the observations from this study, a chart is presented in Fig. 10, which illustrates the regimes where which mode will be present and not. This chart is valid for all the burner configurations once the onset of oscillations has started.

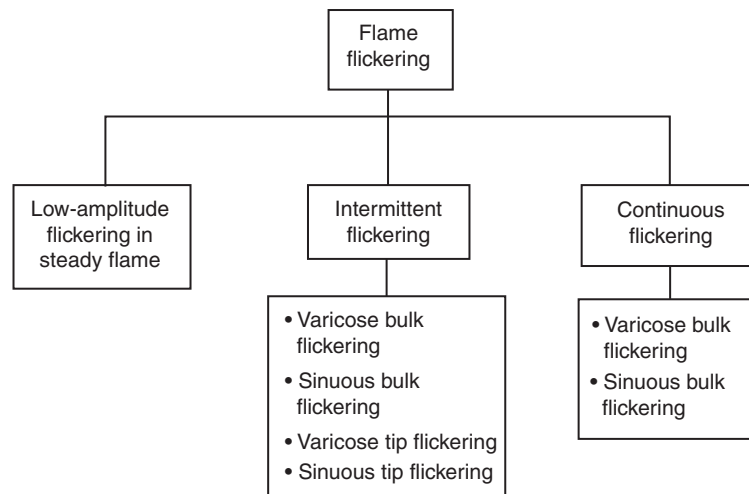


Figure 10: Tree representation of various modes of flame flickering.

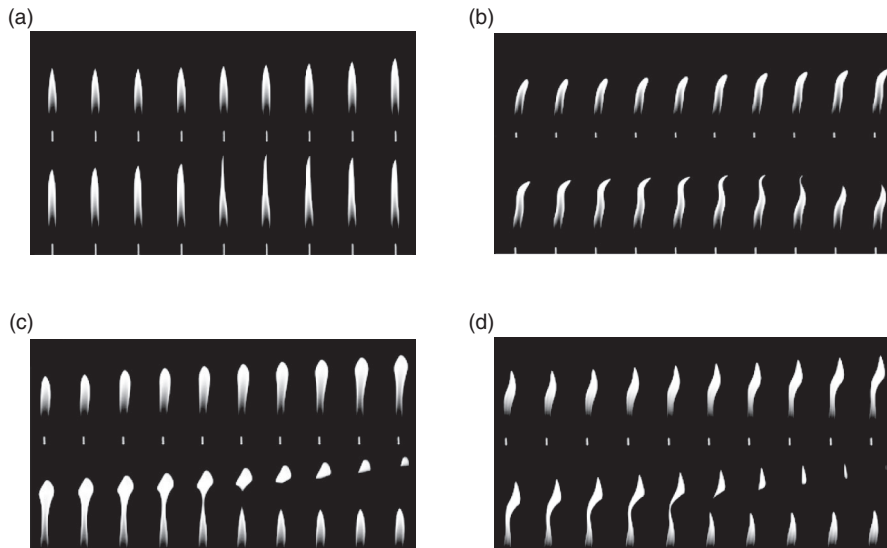


Figure 11: Various modes in intermittent flame flickering in a orifice burner flame for fuel flow rate of 370 mlpm; (a) varicose tip flickering, (b) sinuous tip flickering, (c) varicose bulk flickering and (d) sinuous bulk flickering.

It can be noted that all the four modes of oscillations are observed in the intermittent flickering regime. To describe these, typical cases are presented subsequently. All these four modes of oscillations are illustrated in Fig. 11 for the case of the orifice burner with a fuel flow rate of 370 mlpm ($Re = 137$) with the help series of images extracted at different time periods. Figures 11(a) and 11(b) show the tip flickering modes. Figure 11(a) shows the varicose mode and Fig. 11(b) shows the sinuous mode. Similarly, Figs. 11(c) and 11(d) show the varicose and sinuous modes, respectively, in the bulk flickering. During the onset of intermittent flickering, a steady flame first transforms to the tip flickering mode (either sinuous or varicose). Then, it gradually transforms into the bulk flickering mode, where a portion surrounding the flame tip is chopped off from the main flame. Subsequently, for another given time-period, the flame transits back to the tip flickering mode and settles down as a steady flame for some time, and this process continues. To further demonstrate the randomness of the fluctuations in this regime, flame height data has been extracted for the case of the orifice burner, for the fuel flow rate of 350 mlpm ($Re = 130$), which is in its intermittent flickering regime. This has been plotted in Fig. 12 for a time-period of 4 s. It is observed that the variation in the height of the flame is almost steady for some time (11 s to 12 s) initially, and the gradual onset of oscillations in the flame height is observed after that period. The amplitude of the oscillations in the height of the flame grows for some time and then decreases. During this oscillatory period, both tip as well as bulk flickering can be

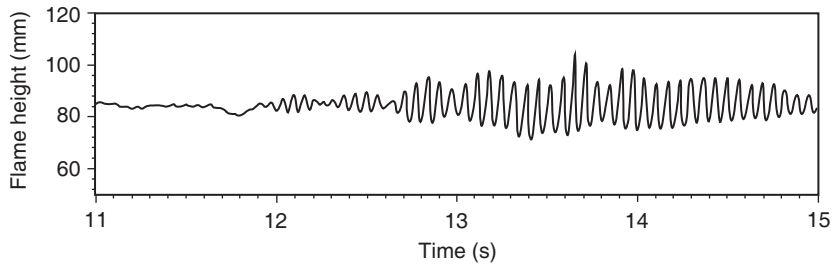


Figure 12: Onset and closure of intermittent flickering in orifice burner.

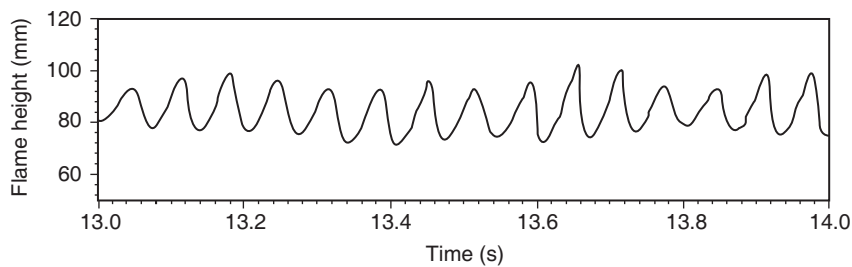


Figure 13: Tip and bulk flickering modes in the intermittent flickering regime for orifice burner.

observed. The major difference in the flame-height variation in tip and bulk flickering modes is the fact when the flame height reduces, it will be gradual for tip flickering and much rapid for bulk flickering. These are clearly indicated in Fig. 13, which presents the flame-height data between 13 s to 14 s.

3.3.3. Effect of burner configuration in intermittent flickering regime

A comparison of the behaviors of the flames from three burners in the intermittent flickering regime is further analyzed. An integrated value of intermittency equal to 25% is considered as the common parameter and the fuel flow rates for the three burners are chosen according to that. As per this criterion, for the pipe burner, the fuel flow rate is 250 mlpm ($Re = 92$), for nozzle burner, the fuel flow rate is 270 mlpm ($Re = 100$) and for the orifice burner, the fuel flow rate is much higher and is equal to 350 mlpm ($Re = 130$). The flame height data is plotted in Fig. 14. As a result of differences in the fuel flow rates, the average flame height is different between the cases; there is a significant increase in the flame height for orifice burner due to much higher fuel flow rate for this case. Intermittent flame flickering can be observed from Fig. 14(a) in between the time instants around 18 s to around 60 s for the pipe burner (inset 1 in Fig. 14). After this, no significant oscillations are observed for this case. Separated intermittent flickering regimes are observed in the case of nozzle burner as shown in Fig. 14(b). Oscillations start around 47 s (inset 2) and again around 137 s (inset 3), and

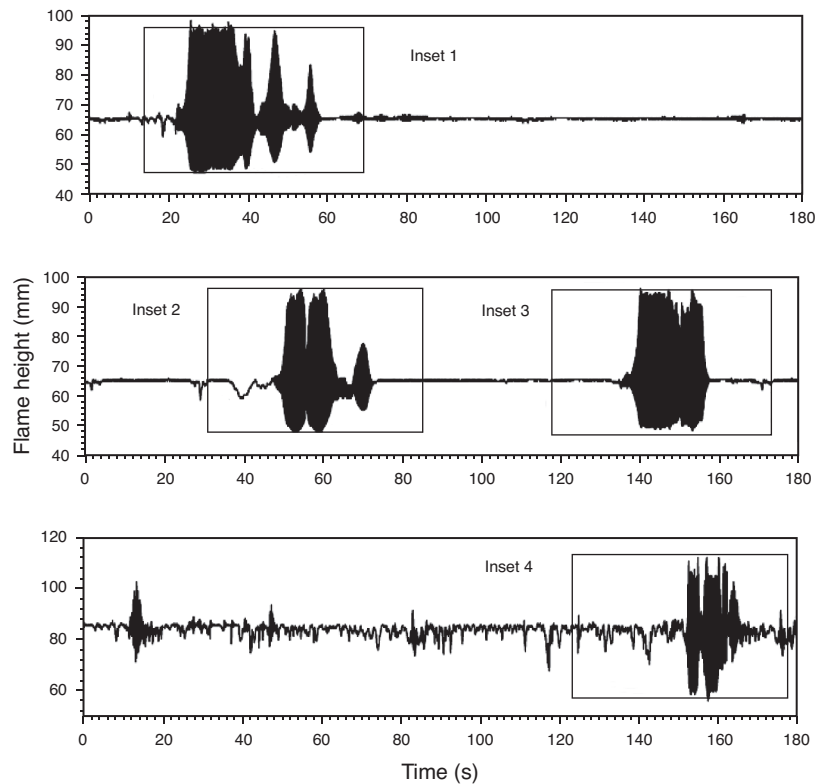


Figure 14: Flame height data when 25% intermittency is observed for (a) pipe burner (250 mlpm; $Re = 92$), (b) nozzle burner (270 mlpm; $Re = 100$) and (c) orifice burner (350 mlpm; $Re = 130$).

are observed for approximately 20 s in each time period. For the orifice burner, which is shown in Fig. 14(c), overall there are oscillations with notable amplitudes throughout the observation time. However, by discounting the low amplitude oscillations, two distinct intermittent oscillatory time periods are observed with significant changes in the amplitudes, one starting around 10 s, lasting for around 8 s, and another starting around 147 s and lasting for around 25 s. Only the 25 s duration, as shown by inset 4, is further analyzed.

FFT of the flame height data shown in the insets in Fig. 14 is carried out. Figure 15 shows the FFT spectra for the four insets. It is observed that for all burners the dominant frequency remains almost constant having a value in between 13 Hz to 14 Hz. Further, Figs. 15(b) and 15(c) show that, for nozzle burner with separated intermittent flickering regimes (insets 2 and 3), even though the flickering frequency remains almost the same, the amplitude varies notably. This shows that the intermittent fluctuations do not follow any given trend.

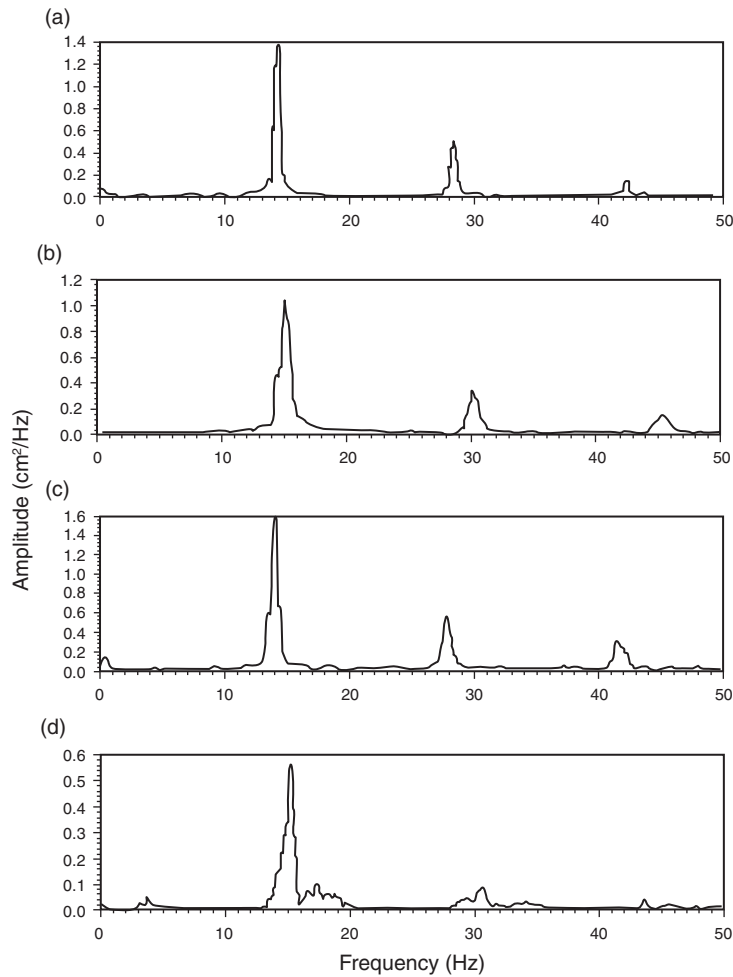


Figure 15: FFT for the flame height data in Fig. 14 for (a) inset 1, (b) inset 2, (c) inset 3 and (d) inset 4.

3.4. Continuous flickering regime

After the onset of the oscillatory regime, as the fuel flow rate is increased gradually, at a certain fuel flow rate, depending on the burner configuration, the flame starts to oscillate continuously. As shown in Fig. 16, only bulk flickering mode is observed in the continuous oscillation regime; flickering can be either varicose or sinuous. The height of the flame increases gradually and the tip of the flame gets separated at a certain height of the flame, and moves up as a flame puff. This imparts a sudden reduction in the height of the flame. The height of the flame increases again from the same position and this phenomenon continues.

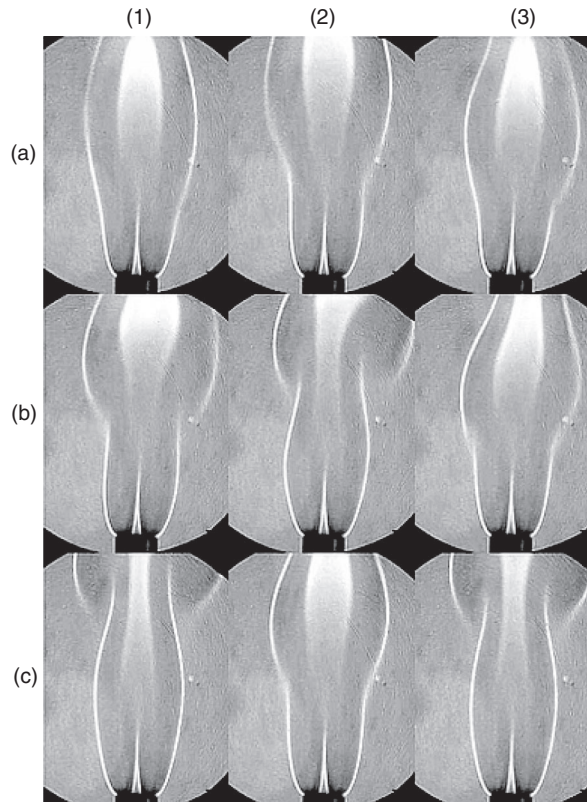


Figure 16: Shadowgraph images illustrating varicose bulk flickering and sinuous bulk flickering modes for the orifice burner for a fuel flow rate of 610 mlpm ($Re = 226$).

3.4.1. Switching of flame flickering modes in bulk oscillation regime

For a jet flame emerging from a circular port, under steady fuel supply rate, the entrainment is expected to be axisymmetric, with symmetrical vortices generated around the flame. This would initiate the varicose flickering mode. However, based on the fuel flow rate, it is observed that after the flame grows to a given height asymmetry can develop and the flame can start to flicker in the sinuous mode. For an orifice burner with a fuel flow rate of 610 mlpm ($Re = 226$), which is in the continuous flickering regime, varicose bulk flickering and sinuous bulk flickering are shown in Figs. 16(a) and 16(b), respectively. The shadowgraph images shown in a given row are captured at a regular time interval of 0.0033 s. Shadowgraphs in Fig. 16 further illustrate the mode switching phenomenon from varicose bulk flickering to sinuous bulk flickering. It is observed in the experiments that the varicose bulk flickering mode is the natural mode of flame flickering because it is the one which is first initiated. The symmetry of the

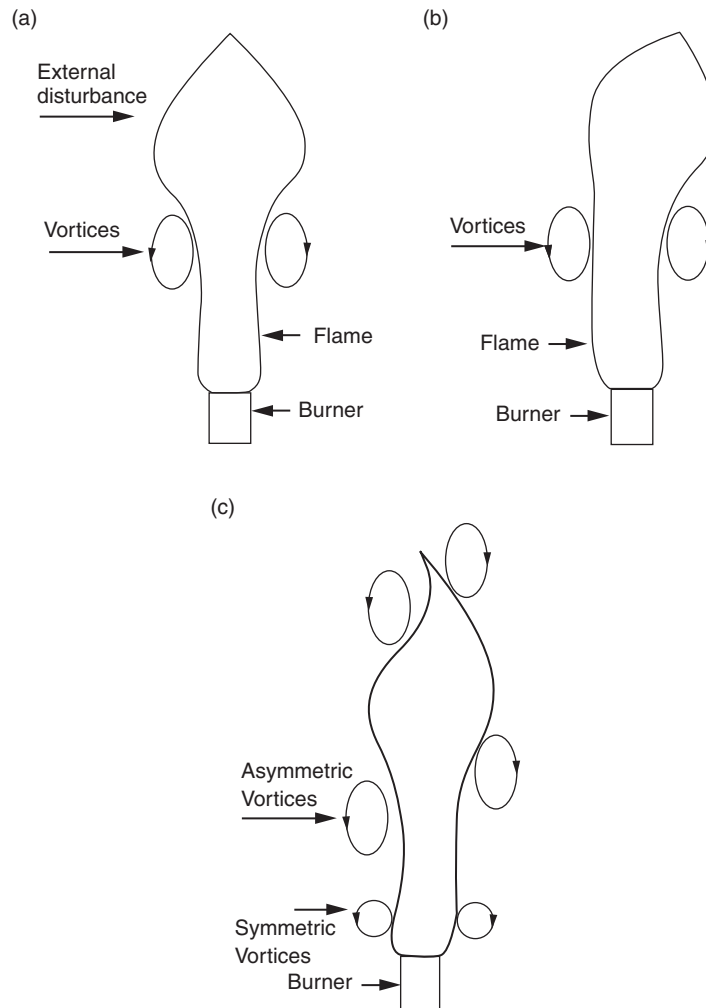


Figure 17: Schematic representation of the mode switching phenomenon (a) varicose flame flickering, (b) asymmetric flame due to external disturbance and (c) damping of sinuous mode by symmetric vortices near the burner exit.

varicose mode is due to the formation of symmetrical vortices around the flame and their interaction with the flame surface. The mode switching from varicose to sinuous occurs due to external disturbances on the flame that result in slight tilting the flame tip asymmetrically. The flames in the varicose mode of flickering, as shown in (a, 1), (a, 2) in Fig. 17, has symmetrical plume (preheat region) around its surface, throughout its height. A slight lateral shift of its tip away from the flame axis occurs as shown in (a,

3), due to any external disturbance. This is shown schematically in Figs. 17(a) and 17(b); the symmetric flame is subjected to asymmetric external disturbance and becomes asymmetric. This results in asymmetric heating around the flame. Consequently, the strength of buoyancy increases on the right side of the flame towards which the flame has tilted, as compared to the left side. As a result, the right side vortex intensifies and rises faster as shown in the image (b, 1) in Fig. 16, causing the thermal plume around the flame in the right hand side to detach. This further intensifies as observed in the image (b, 2) in Fig.16. In this manner, the flame shifts to sinuous bulk flickering mode.

The rise of symmetrical the vortices which are formed near the burner rim tries to damp the sinuous bulk flickering mode as shown in the image (b, 3) and (c, 1) in Fig. 16. By this process, the flame becomes aligned again with respect to the burner axis, as shown in image (c, 3) in Fig. 16. All the vortices become symmetric and the oscillation mode shifts from sinuous to varicose. This is shown schematically in Fig. 17(c). These processes continue. Mode switching from the sinuous bulk flickering mode to the varicose bulk flickering mode is clearly observed from the series of images (b, 3) to (c, 3) in Fig. 16. The flame tip separation is not captured as the flame height is larger than the height up to which the shadowgraph image has been captured.

3.4.2. Flame height and flickering frequency

The temporal variations in the flame heights from three burners at a fuel flow rate of 610 mlpm ($Re = 226$) is shown in the Fig. 18. The maximum and the minimum lengths of the flame are seen to continuously vary with respect to time. The variations in the flame heights are almost similar for pipe and nozzle burners, even though the pipe burner produces higher flame height when compared to the nozzle burner. On the other hand, the temporal variation of the flame height is seen to be quite random for the orifice burner, even though it produces the least average flame height. This is due to the fact that the flow field out of the orifice is very sensitive to the disturbances and leads to the formation of vortices at various growth rates.

FFT analysis is carried out for the flame height data of three burners presented in Fig. 18. The FFT plots are presented in Fig.19. These results show that there is no significant effect of burner configurations on the natural flickering frequency of the flame in the continuous oscillation regime as well. The natural flickering frequencies for all the cases are found to be in the range of 13.5 ± 1 Hz. It is evident from Fig. 19 that harmonics are present in the frequency spectra. The spectra for the nozzle burner (Fig. 19b) show that the flame flickering is associated with pure sinusoidal waves, indicated by the clear peaks. In the case of orifice, pipe burners, cluster of peaks are observed, indicating some randomness.

3.4.3. Variation of flickering frequency with respect to fuel flow rate

The dominating flickering frequency is another principle characteristic of the flickering flame. This parameter is closely related to the dominating frequency at which vortices generate from the burner tip. An attempt is made to estimate the dominating natural flickering frequency of the oscillating flame as a function of the fuel flow rate and

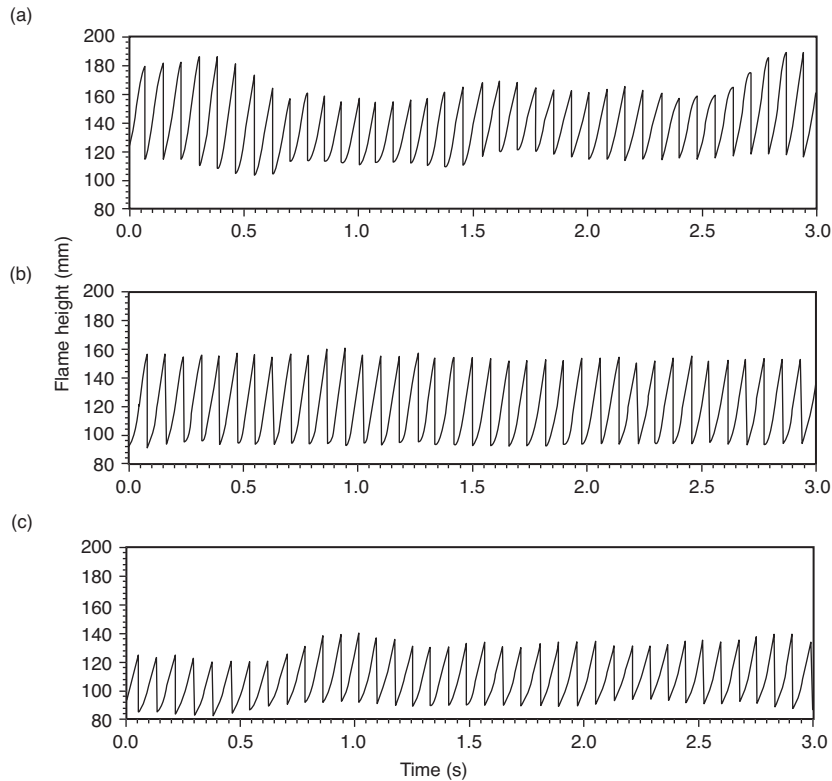


Figure 18: Flame height variation with respect to time at the fuel flow rate of 610 mlpm ($Re = 226$) for (a) pipe burner, (b) nozzle burner and (c) orifice burner.

compare that between all the three burners. The fuel flow rates are in the range of 510 mlpm to 610 mlpm, which is the continuous flickering regime for the all three burners. The results are shown in 3D FFT plots in Fig. 20.

The results show that the fuel flow rate or the burner configuration does not affect the dominating natural frequency of a continuously flickering flame. However, an increase in the fuel flow rate results in an increase of the amplitude of the flickering flame. The rate at which vortices generate from the burner tip remains almost the same and the amplitude of oscillation increases with increasing fuel flow rate as a result of increase in the overall flame length with fuel flow rate.

3.4.4. Variation of flame scale parameters

For an oscillating flame, certain length-scale parameters will be useful to understand the oscillation behavior. These parameters are schematically shown in Fig. 21. The parameters L_{\max} and L_{\min} are the average values of the maximum and the minimum heights measured from the burner exit to the tip of the visible flame during a given time period. The parameter L_p is the peak-to-peak amplitude of flame oscillation, or in other words, it is the difference between L_{\max} and L_{\min} . Comparisons of L_{\max} , L_{\min} and L_p are made between the

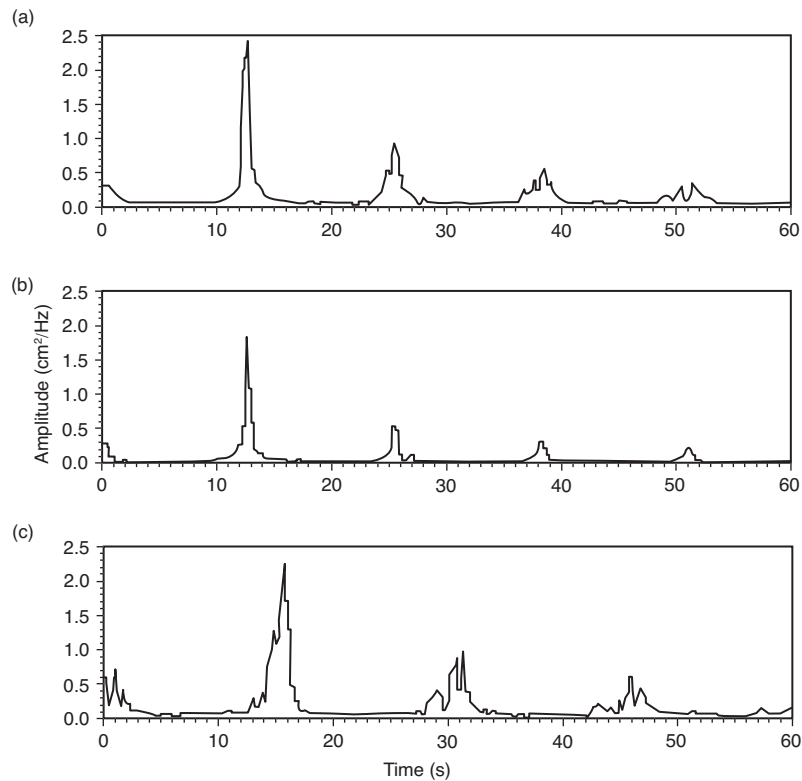


Figure 19: FFT spectra of flame height at the fuel flow rate of 610 mlpm ($Re = 225$), for (a) pipe burner, (b) nozzle burner and (c) orifice burner.

three burners for the fuel flow rates in the range of 490 mlpm to 610 mlpm, which impart continuous oscillations to the flames in all the cases. The length-scale parameters have been averaged over a time span of six seconds and are presented in Fig. 22.

It is clear that L_{\max} and L_{\min} increases with respect to the fuel flow rate, irrespective of the burner configuration. Due to the higher momentum, the average flame height increases and this is one of the basic characteristics of the laminar jet diffusion flame. It is noted that the values of average L_{\max} and L_{\min} are almost of the same order in the cases of pipe and nozzle burners, and are notably smaller for the orifice burner.

Further, L_p remains almost a constant with the fuel flow rate. The value of L_p is almost the same for pipe and nozzle burners and it is slightly lower for the orifice burner. This clearly indicates that there is a certain height where the fuel can be completely consumed to a critical extent based on the fuel flow rate. Within that distance, the vortex from the surrounding flow field cannot interact with the flame zone, so as to change its characteristics. The values of L_{\max} and L_{\min} for the flame from the orifice burner are lesser than the other two cases for all flow rates due to the maximum

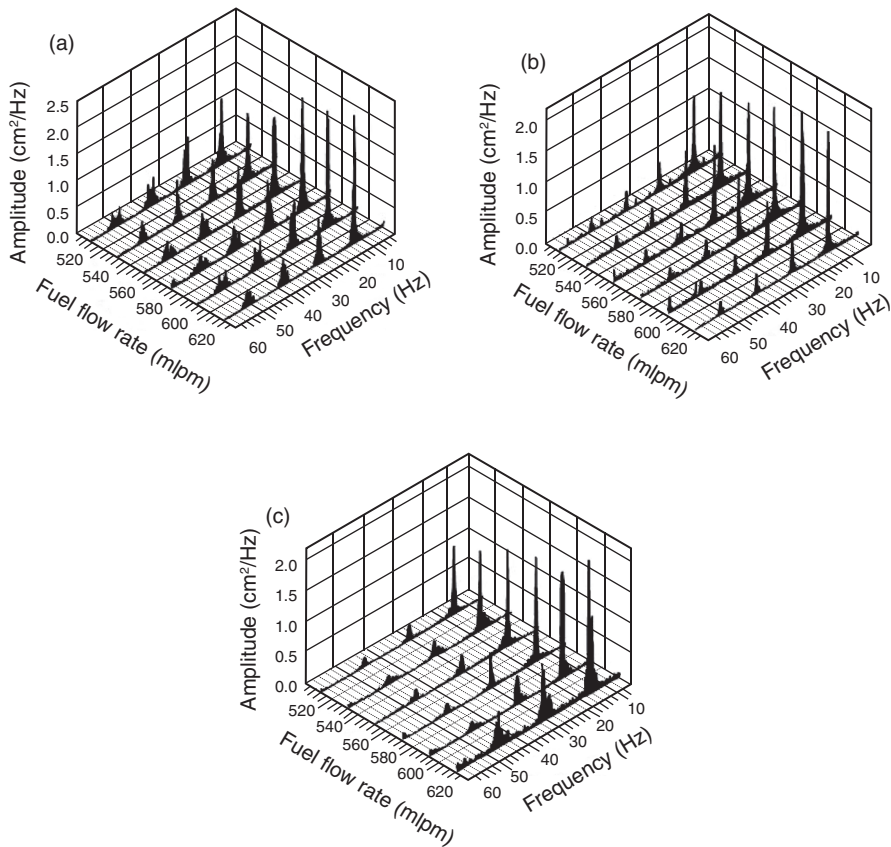


Figure 20: Comparison of dominating flickering frequency as a function of fuel flow rate for (a) pipe burner, (b) nozzle burner and (c) orifice burner.

mixing ability of the orifice jet with the ambient fluid. The variation of peak-to-peak amplitude is around 50 mm for orifice case, whereas it is equal to around 60 mm for both nozzle and straight pipe case.

4. CONCLUSIONS

The experimental investigations on the burner configurations on diffusion flames show that, the orifice burner exhibits an overall different behavior as compared to pipe and nozzle burners. Basically the mixing characteristics of the jet are significantly improved due to the presence of the orifice plate. The enhanced mixing effect of the orifice is clearly reflected in the temperature distribution and thermal plume width around the flame compared to other two burners. The performances of nozzle and pipe burners are almost the same. The shadowgraph images show that the preheat plume is farther away in the case of the orifice burner (by around 13%) as compared to other burners, as a result of higher entrainment of the ambient air for that case.

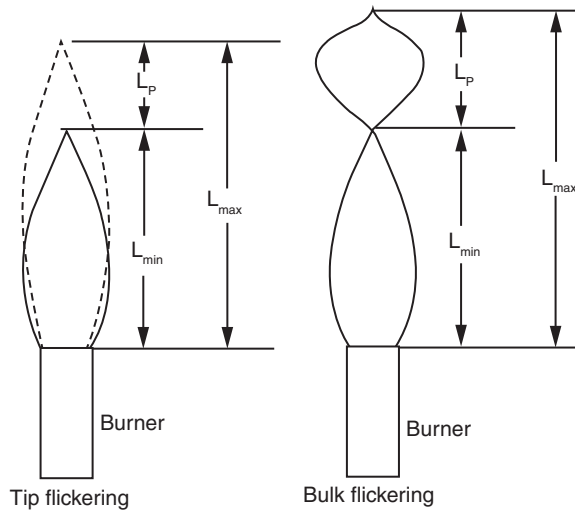


Figure 21: Schematic diagram defining the flame length-scale parameters.

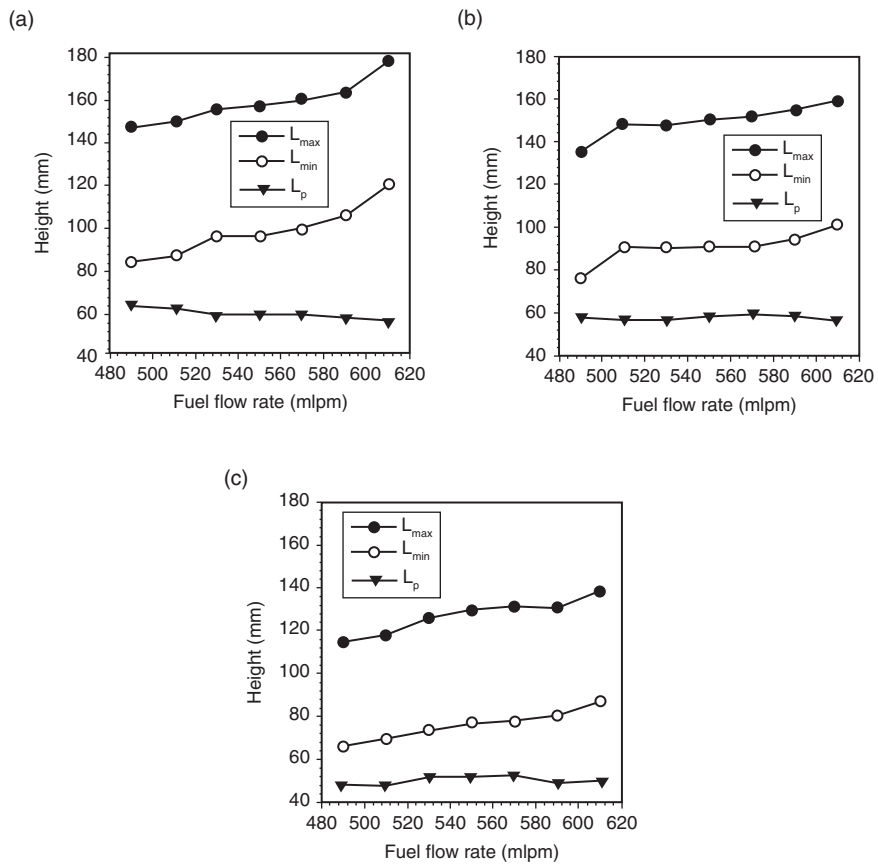


Figure 22: Variation of length-scale parameters of the flames with respect to fuel flow rate for (a) pipe burner, (b) nozzle burner and (c) orifice burner.

Even in steady burning regime, the orifice burner shows higher radial temperature distribution and shorter flame height. From the FFT analysis on the flame height data, it has been observed that the dominating frequency in the natural oscillation regime remains almost within a small range, around 12.5 Hz to 15 Hz, for all the burners, irrespective of the fuel flow rate and burner configuration. This observation is consistent with the reports available in literature. The time-averaged flame length-scale parameters, such as the maximum and the minimum heights, increase with respect to the fuel flow rate showing that in the laminar regime the average flame height increases with the fuel flow rate. The difference in the maximum and minimum flame heights remains almost constant.

To further investigate the reasons for the observed variations, velocity field measurements using techniques such as PIV, HWA and LDV can be attempted. Numerical simulations of natural flickering in the jet diffusion flames can be carried out. A DNS like grid and transient simulations with detailed chemistry are required to achieve this.

REFERENCES

- [1] Grant, A.J. and Jones, J.M., Low-frequency diffusion flame oscillations, *Combustion and Flame*, 1975, 25, 153–160.
- [2] Chamberlin, D.S. and A. Rose, The flicker of luminous flames, *Proceedings of the Symposium on Combustion*, 1948, 1-2, 27–32.
- [3] Hamins, A., Yang, J.C. and Kashiwagi, T., An experimental investigation of the pulsation frequency of flames, *Symposium (International) on Combustion*, 1992, 24, 1695–1702.
- [4] Maxworthy, T., The Flickering candle: transition to global oscillation in a thermal plume, *Journal of Fluid Mechanics*, 1990, 390, 297–323.
- [5] Li, J. and Zhang, Y., Fuel variability effect on flickering frequency of diffusion flames, *Frontier Energy Power Eng. China*, 2009, 3, 134–140.
- [6] Sato, H., Amagai, K. and Arai, M., Flickering frequencies of the diffusion flames observed under various gravity fields, *Proceedings of the Combustion institute*, 2000, 28, 1981–1987.
- [7] Darabkhani, H.G. and Zhang, Y., Methane diffusion flame dynamics at elevated pressures, *Combustion Science and Technology*, 2010, 182, 231–251.
- [8] Darabkhani, H.G., Wang, Q., Chen, L. and Zhang, Y., Impact of co-flow air on buoyant diffusion flames, *Energy conservation and Management*, 2011, 52, 2996–3003.
- [9] Huang, H.W., Wang, Q., Tang, H.J., Zhu, M. and Zhang, Y., Characterisation of external acoustic excitation on diffusion flames using digital colour image processing, *Fuel*, 2012, 94, 102–109.
- [10] Kimura, I., Stability of Laminar Jet Flames, *Symposium (International) on Combustion*, 1965, 10, 1295–1300.

- [11] Toong, T.Y., Richard, S.F., John, S.M. and Griffin, A.Y., Mechanism of Combustion Instability, *Symposium (International) on Combustion*, 1965, 10, 1301–1313.
- [12] Buckmaster, J. and Peters, N., The Infinite Candle and its Stability- A paradigm for Flickering Diffusion Flames, *Symposium (International) on Combustion*, 1988, 21, 1829–1836.
- [13] Davis, R.W., Moore, E.F., Roquemore, W.M., Chen, L.D., Vilimpoc, V. and Goss, L.P., Preliminary results of a Numerical-Experimental study of Dynamic structure of a Buoyant Jet Diffusion Flame, *Combustion and Flame*, 1991, 83, 263–270.
- [14] Katta, V. R. and Roquemore, W.M., Role of Inner and Outer Structures in a Transition Jet Diffusion Flame, *Combustion and Flame*, 1993, 92, 274–282.
- [15] Boulanger, J., Laminar round jet diffusion flame buoyant instabilities: Study on the disappearance of varicose structures at ultra-low Froude number, *Combustion and Flame*, 2010, 157, 757–768.
- [16] Cetegen, B.M. and Dong, Y., Experiments on the instability modes of buoyant diffusion flames and effects of ambient atmosphere on the instabilities, *Experiment in Fluids*, 2000, 28, 546–558.
- [17] Manikantachari, K.R.V., Raghavan, V. and Srinivasan, K., Natural Flickering of Methane Diffusion Flames, *World Academy of Science Engineering and Technology*, 2011, 5, 1925–1930.
- [18] Kanthasamy, C., Raghavan, V. and Srinivasan, K., Effect of low frequency burner vibrations on the characteristics of jet diffusion flames, *International Journal of Spray and Combustion Dynamics*, 2012, 4, 77–96.